arXiv:1303.4421v2 [physics.soc-ph] 20 Mar 2013

Remote Synchronization in Complex Networks

L.V. Gambuzza,[1] A. Cardillo,[2,3] A. Fiasconaro,[2,4] L. Fortuna,[1] J. Gómez-Gardeñes,[2,3] and M. Frasca[1,*]

[1]*Dipartimento di Ingegneria Elettrica, Elettronica e Informatica, University of Catania, I-95125 Catania (Italy).*
[2]*Departamento de Física de la Materia Condensada, University of Zaragoza, Zaragoza 50009, Spain*
[3]*Institute for Biocomputation and Physics of Complex Systems (BIFI), University of Zaragoza, Zaragoza 50018, Spain*
[4]*Instituto de Ciencia de Materiales de Aragón, CSIC–University of Zaragoza, Zaragoza 50009, Spain*

(Dated: March 21, 2013)

We show the existence of a novel dynamical state called remote synchronization in general networks of coupled oscillators. This state is characterized by the synchronization of pairs of nodes that are not directly connected via a physical link or any sequence of synchronized nodes. This phenomenon cannot be observed in networks of phase oscillators as its underlying mechanism is the modulation of the amplitude of those intermediary nodes between the remotely synchronized units. Our findings thus show the ubiquity and robustness of these states and bridge the gap from their recent observation in simple toy graphs to complex networks.

Synchronization constitutes one of the most paradigmatic examples of emergence of collective behavior in natural, social and man-made systems [1–3]. Its ubiquity relies on the general framework in which it occurs: the interaction between two or more nonidentical dynamical units that, as a consequence, adjust a given property of their motion. As coupling between units increases, synchronization shows up as a collective state in which the units behave in a coordinate way. Synchronization phenomena span across many life scales, ranging from the development of cognitive tasks in neural systems [4] to the onset of social consensus in human societies [5].

The ubiquity of synchronization in real systems together with the recent discovery [6–8] of their real architecture of interactions has motivated its study when units are embedded in a complex network [9]. In this way, each unit is represented as a node of a network while it only interacts with those adjacent units, *i.e.* those directly coupled via an edge. In the last decade many studies have unveiled the impact that diverse interaction topologies have on the onset of synchrony [10–14] and its stability [15–18]. In addition, related issues such as that of adaptive networks, in which the interaction pattern changes according to the degree of synchronization of the system, have also attracted the attention of the community [19–22].

The former studies mainly rely on the study of coupled phase oscillators, such as the Kuramoto model [23, 24], which produces globally synchronized systems as a result of the direct interaction of pairs of adjacent units. However, it has been recently found [25] that, for more general oscillator models (in which both amplitude and phase are dynamical variables) such as the Stuart-Landau model [2], two oscillators, that are not directly linked but are both connected to a third unit, can become synchronized even if the third oscillator does not synchronize with them. This novel phenomenon, coined *remote synchronization*, relies on the modulation of the amplitude parameter of an intermediary node allowing the passage of information between two of its neighbors for their synchronization, even when the former is not synchronized with them. Thus, this tunnel-like mechanism is out of reach in ensembles of phase oscillators.

Remote synchronization has been found to occur in very specific and simple topologies such as star-like networks in which the central node has a natural frequency different from that of the leaves. Within this particular setting it was numerically and experimentally shown [25] that leaves become mutually synchronized without the need of the synchronization of the central node. In this Letter, we aim at showing that remote synchronization is not limited to the particular configuration of a star-like motif or a tight specification of the node frequencies. To this end, we show its ubiquity and robustness in the general case of complex networks.

The dynamical model consists of a network of N coupled Stuart-Landau oscillators [2]. Each node i is characterized by two variables, $(x_i, y_i)^T$, whose dynamical evolution is as follows:

$$\begin{pmatrix} \dot{x}_i \\ \dot{y}_i \end{pmatrix} = \begin{pmatrix} \alpha - x_i^2 - y_i^2 & -\omega_i \\ \omega_i & \alpha - x_i^2 - y_i^2 \end{pmatrix} \begin{pmatrix} x_i \\ y_i \end{pmatrix} + + \frac{\lambda}{k_i} \sum_{j=1}^{N} L_{ij} \begin{pmatrix} x_j \\ y_j \end{pmatrix} , \tag{1}$$

where α^2 and ω_i are respectively the amplitude and the (natural) frequency of oscillator i when uncoupled. The second term on the right accounts for the coupling of the dynamics of i with its k_i first neighbors. The strength of the coupling is controlled by λ ($\lambda = 0$ in the uncoupled limit) while $\mathcal{L} = \{L_{ij}\}$ represents the Laplacian of the network defined as: *(i)* for $i \neq j$, $L_{ij} = 1$ when nodes i and j are connected while $L_{ij} = 0$ otherwise, and *(ii)* $L_{ii} = -k_i$.

To study the synchronization properties of system (1) we work with the phase variable of each oscillator, defined as $\theta_i = \tan^{-1}(y_i/x_i)$. Then we can measure the degree of synchronization of any (connected or not) pair of oscillators as:

$$r_{ij} = |\langle e^{i[\theta_i(t) - \theta_j(t)]} \rangle_t| , \tag{2}$$

where $\langle \cdot \rangle_t$ means an average over a large enough time interval. We will consider two nodes as synchronized when $r_{ij} > \delta$, where δ is a constant threshold that we fix to $\delta = 0.8$. Nonetheless, we checked that the results presented are robust as other values of δ yield qualitatively the same outcomes.

Once two nodes i and j are classified as mutually synchronized we label their relationship according to the following three situations: *(i)* i and j are directly connected

---

[*] mfrasca@diees.unict.it

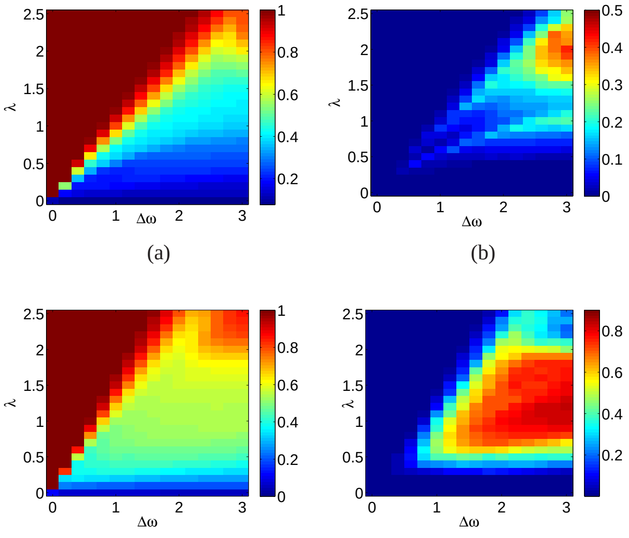

(a) (b)

(c) (d)

FIG. 1. (color online). Evolution of the degree of global synchronization r [panels (a) and (c)] and the number of remotely synchronized nodes n_{RS} [panels (b) and (d)] for SF (upper panels) and ER (bottom panels) networks as a function of the coupling strength λ and the frequency mismatch $\Delta\omega$. In both cases the networks have $N = 100$ and $k = 2$. The other relevant parameters are fixed to $\alpha = 1$, $\omega_l = 1$.

($L_{ij} = L_{ji} = 1$), *(ii)* there is a path of mutually synchronized nodes between them, and *(iii)* none of the former two situations hold. While the first two cases are similar, as both are examples of synchronization through *physical links*, the third case is analogous to the observed remote synchronization in a star-like network, but in the more general context of a complex network. Thus, we define that two nodes i and j are remotely synchronized (RS) when they are synchronized ($r_{ij} > \delta$) and they are not connected by either a direct link or a path of synchronized nodes.

To quantify systematically the extent of remote synchronization we count the number of RS nodes, defined as the number N_{RS} of nodes that appear RS with at least another node in the network. This allows us to introduce the following order parameter: $n_{RS} = N_{RS}/N$, representing the normalized number of RS nodes with respect to the total number of nodes N. Finally, to quantify the importance that remote synchronization has on the dynamics of the system we also measure the global level of synchronization through the usual Kuramoto-like order parameter:

$$r = \frac{1}{N^2} \sum_{i,j=1}^{N} r_{ij} \ . \qquad (3)$$

Note that r takes into account the contribution of both synchronized ($r_{ij} > \delta$) and not synchronized ($r_{ij} \leq \delta$) nodes.

As two well-known paradigmatic network topologies we have analyzed both Erdős-Rényi (ER) and Scale-free (SF) graphs. The former type of networks is characterized by a Poisson distribution $P(k)$ for the probability of finding a node with k contacts while SF graphs show a power-law distribution, $P(k) \sim k^{-\gamma}$. Thus, while in ER graphs most of the nodes are close to the mean connectivity $\langle k \rangle$, SF networks display a large heterogeneity in the number of contacts per node as revealed from the existence of hubs having $k_i \gg \langle k \rangle$. For their construction we have made use of the model introduced in [26] that allows to control the mean connectivity of both networks in order to be exactly the same. In the networks reported in this Letter the size and mean connectivity are fixed to $N = 100$ and $\langle k \rangle = 2$ respectively. Finally, in order to stay close to the framework used in [25] we have considered a bimodal distribution for the natural frequencies of the oscillators so that nodes with high degree (those analogous to the central nodes in a star graph) present a larger frequency, ω_h, than that, ω_l, of less connected (the ones playing the role of leaves in the star topology). In particular, we labeled as hubs those nodes having $k_i > k^*$ [27] and assigned them $\omega_i = \omega_h + \xi_i \omega_h$ while, for the rest of nodes $\omega_i = \omega_l + \xi_i \omega_l$. In the former expressions ξ_i is a random variable uniformly distributed between -0.025 and 0.025.

In Fig. 1 we show the emergence of remote synchronization as a function of the two relevant parameters: the coupling strength λ and the frequency mismatch of the network hubs $\Delta\omega = \omega_h - \omega_l$. In particular, we report the behavior of the global synchronization, r, [panels 1(a) and 1(c)] and the fraction of RS nodes, n_{RS}, [panels 1(b) and 1(d)] for SF (top) and ER (bottom) networks. The results are averaged over 50 different network instances and, for each network we average the results over 10 different realizations of the distribution of natural frequencies.

We find that remote synchronization occurs in both types of networks in a region of parameters characterized by a strong frequency mismatch $\Delta\omega$ and moderate coupling λ. In fact, for low values of the coupling parameter, nodes cannot synchronize (either in a direct or remote way) as observed from the low values of r and n_{RS}. On the contrary, for large values of λ the network is fully synchronized ($r \simeq 1$) and, accordingly, n_{RS} assumes values close to zero since all the nodes are mutually synchronized with their neighbors. As panels 1(a) and 1(c) reveal, the onset of full synchronization requires greater values of the coupling as the frequency mismatch increases. In fact, a large frequency mismatch together with values of coupling under the threshold for complete synchronization favors the onset of remote synchronization, as observed from the behavior of n_{RS} in panels 1(b) and 1(d).

Compared to SF networks, the values of n_{RS} in ER networks are greater, thus indicating that remote synchronization in ER networks involves both a larger number of nodes. Moreover, in ER networks the onset of remote synchronization occurs for lower values of λ. ER and SF networks also show qualitative differences in the appearance of remote synchronization: by keeping fixed $\Delta\omega$ and increasing the value of λ, we find that n_{RS} in SF networks show two peaks, while for ER networks it shows a rise-and-fall behavior.

In both (ER and SF) cases remote synchronization appears as an intermediary state before full synchronization is achieved. However, from the analysis of panels 1(a) and 1(c) one observes that the behavior of r *vs.* λ for a fixed value

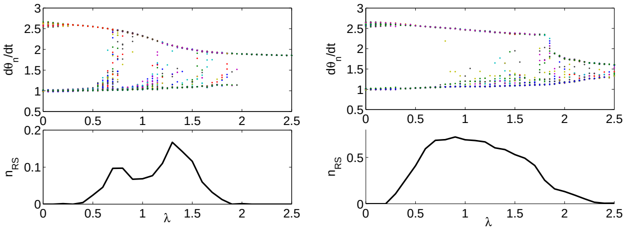

(a) (b)

FIG. 2. (color online). Evolution of the average oscillation frequency of each oscillator and n_{RS} as a function of λ for SF (a) and ER (b) networks. The mismatch of natural frequencies is $\Delta\omega = 1.5$ while the rest of parameters are the same as in Fig 1.

of $\Delta\omega$ is qualitatively different in SF and ER networks. In particular, in ER networks (panel 1(c)) a large plateau around $r \simeq 0.5$ is set in the region where remote synchronization shows up. In this region, the increase of λ does not contribute to the overall synchronization level, but to a redistribution of the average oscillation frequencies of the network nodes.

This is evident in Fig. 2, where the average values (over the simulation time T) of the instantaneous frequency of each oscillator are reported along with the parameter n_{RS}. The results are obtained by increasing λ adiabatically from $\lambda = 0$ so that the system starts from a bimodal distribution as dictated by the configuration for the natural oscillations. As λ increases, the gap between the two main frequencies values of the bimodal distribution decreases until the network reaches full synchronization and the nodes oscillate at a common frequency. The readjustment of frequencies reveals that, for some values of the coupling, the system undergoes a strong reorganization, pointed out by the spread of the oscillation frequencies between the two extreme values. This readjustment coincides with the peaks displayed by n_{RS} in both SF and ER networks. However, the readjustment seems to occur faster in SF networks for which the plateau of r is not observed.

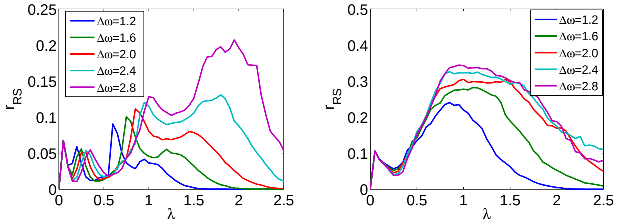

(a) (b)

FIG. 3. (color online). Evolution of the fraction or RS links, r_{RS}, in SF (a) and ER (b) networks as a function of the coupling strength λ. The remaining parameters are set as in Fig. 1.

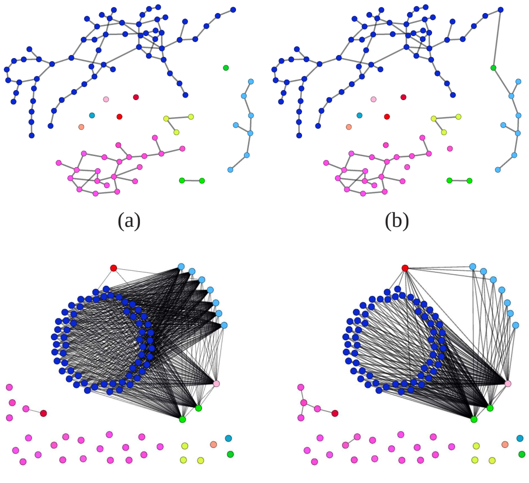

(c) (d)

FIG. 4. (color online). Evolution of components of physically (a)-(b) and remotely (c)-(d) synchronized nodes in an ER network with $\Delta\omega = 2.8$, when λ is increased by adiabatic continuation from $\lambda = 1.65$ (a)-(c) to $\lambda = 1.70$ (b)-(d). Nodes are colored according to the physically synchronized component they belong to when $\lambda = 1.65$, *i.e.* in (a). The remaining parameters are the same as in Fig 1.

To gain more insight on the relation between the regime of remote synchronization and the onset global synchrony we now consider the analysis of all synchronized pairs and its partition into those corresponding to remote synchronization and those for which a synchronized physical connection (either a direct link or a path of synchronized nodes) exists. To this aim, we define $\eta_{ij} = 1$ if nodes i and j are connected either by a physical link or by a path of synchronized nodes and $\eta_{ij} = 0$, otherwise. We then introduce the following parameters:

$$r_P = \frac{\sum_{i,j=1}^{N} \eta_{ij} H(r_{ij} - \delta) r_{ij}}{\sum_{i,j=1}^{N} H(r_{ij} - \delta)} \,, \tag{4}$$

and

$$r_{RS} = \frac{\sum_{i,j=1}^{N} (1 - \eta_{ij}) H(r_{ij} - \delta) r_{ij}}{\sum_{i,j=1}^{N} H(r_{ij} - \delta)} \,, \tag{5}$$

where $H(x)$ is the Heaviside function. Thus, r_P and r_{RS} represent the fraction of synchronized links due to a physical or remote connection, respectively. Obviously, as $r_P + r_{RS} = 1$, it is enough to report the behavior of r_{RS}.

In Fig. 3 we show the evolution of r_{RS} vs. λ for several values of $\Delta\omega$. The presence of two peaks in the evolution of r_{RS} in SF networks reveals a similar behavior to that found for n_{RS}. As $\Delta\omega$ increases, the percentage of RS links increases and the two peaks shift towards increasing values of λ. On the other hand, for ER networks the percentage of RS links is higher than in SF networks and r_{RS} shows, as in the case of n_{RS}, a rise-and-fall trend. The fall in the number of RS links points out that the network is able to recruit physical links to get synchronized and thus those regions that appeared as RS become merged into a single component made of physically synchronized links.

To visualize the progressive substitution of RS links by physical ones in the path towards full synchronization we show in Fig. 4 for an ER network (with $\Delta\omega = 2.8$) snapshots of both remotely and physically synchronized links for two values of the coupling λ. In Figs. 4(a) and 4(c) we plot

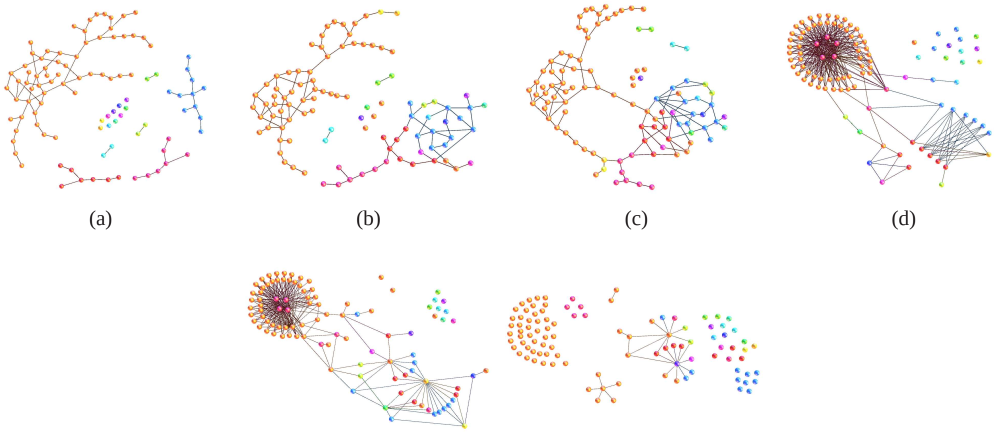
(a) (b) (c) (d)

(e) (f)

FIG. 5. Evolution of components of physically (a),(b), (c) and remotely (d),(e), (f) synchronized nodes in an ER network with $\Delta\omega = 1.5$ and $\langle k \rangle = 2$, when λ is adiabatically increased. Nodes are colored according to the component to which they belong in (a) and, then, represented with the same colors in (b)-(f). The networks correspond to the following value of λ: (a)-(b) $\lambda = 1.75$; (c)-(d) $\lambda = 1.80$; (e)-(f) $\lambda = 1.85$.

two networks corresponding to physically and remotely synchronized links respectively when $\lambda = 1.65$. In this case the network is divided into several clusters of physically synchronized nodes (the color of the nodes corresponds to the cluster of physically synchronized links they belong to) and some nodes of these clusters appear remotely synchronized with nodes belonging to different clusters [as shown in Fig.4(c)]. When λ is increased to $\lambda = 1.70$, two of these clusters merge together [Fig. 4(b)] through two physically synchronized links that connect each cluster to a new node synchronized to each of them. Thus, at $\lambda = 1.70$ two communities, that were remotely synchronized at $\lambda = 1.65$, fuse into a single one and, as a consequence, those RS links between the nodes of the two communities reported for $\lambda = 1.65$ in Fig. 4(c) disappear at $\lambda = 1.70$ [Fig. 4(d)]. A further example of the merging of RS clusters is shown in Fig. 5). We consider an ER network with $\Delta\omega = 1.5$ and $< k_n >= 2$, when λ is increased with continuation from $\lambda = 1.75$ to $\lambda = 1.85$. For $\lambda = 1.75$ the network is divided into four main components of physically synchronized nodes plus some small communities and isolated nodes (Fig. 5(a)). The analysis of the components of RS nodes (Fig. 5(d)) reveals that the there are RS links between the four communities. In fact, increasing the coupling to $\lambda = 1.80$ three of these communities merge (Fig. 5(b)) and, correspondingly, the RS links between these communities disappear (Fig. 5(e)). Finally, a further increase of λ ($\lambda = 1.85$ in Fig. 5(c)) leads to the aggregation of the fourth community (the bigger one) to the previous ones. Also in this case, amost all the RS links disappear (Fig. 5(f)) and very few RS links are observed for $\lambda = 1.85$.

Summarizing, in this Letter we have shown that remote synchronization can be observed in general complex networks. This phenomenon relies on the mutual synchronization of pairs of uncoupled nodes. Each remotely synchronized pair of nodes are thus physically connected through an intermediary node (not synchronized with them) or a sequence (path) of intermediary nodes. Although its original formulation was restricted to a rather particular and simplistic setup, a star graph, here we have extended its formulation to the general case of complex networks such as Erdős-Rényi and Scale-free graphs of coupled oscillators having amplitude and phase as dynamical variables. The addition of amplitude as a dynamical variable, in contrast with the typical framework of networks of coupled phase-oscillators, provides the observation of remote synchronization, a mechanism anticipating synchronization by physical links in networks with heterogeneous distribution of natural frequencies.

It is important to note that remote synchronization is not observed for ensembles of phase oscillators as its underlying mechanism is the modulation of the amplitude of those intermediary nodes allowing the information transfer between uncoupled pairs of nodes. On the contrary, when similar settings are applied to phase oscillators a different phenomenon is observed, namely that of *explosive synchronization* [14] in which the typical second-order synchronization transition transforms into a first-order one. In its turn, remote synchronization appears as a rather robust state prior the onset of global synchronization since for a wide range of coupling strengths almost all the nodes are remotely synchronized with, at least, another one while the level of global synchronization remains small. Thus, our results open the door for experimental observations of this novel state in which the existence of a synchronized pair cannot be associated to a given physical interaction through a single link of the network and highlight the important difference between the real (*i.e.* associated to physical links) and the functional (*i.e.* emerging from synchronization) connectivity of a network.

ACKNOWLEDGMENTS

Support came from the Spanish MINECO (projects FIS2011-25167 and FIS2011-14539-E) and the Comunidad de Aragón (FENOL group). J.G.G. is supported by MINECO through the Ramón y Cajal program.

[1] S.H. Strogatz, Physica D **143**, 1 (2000).

[2] Pikovsky, A., Rosenblum, M. & Kurths, J. *Synchronization: a Universal Concept in Nonlinear Sciences* (Cambridge University Press, 2003).

[3] S. Boccaletti, *The Synchronized Dynamics of Complex Systems* (Elsevier, 2008).

[4] E. Bullmore and O. Sporns, Nature Reviews Neuroscience **10**, 186 (2009).

[5] A. Pluchino, V. Latora, A. Rapisarda, Internat. J. Modern Phys. C **16**, 515 (2005).

[6] S. Boccaletti, V. Latora, Y. Moreno, M. Chavez and D. U. Hwang. Phys. Rep. **424**, 175–308 (2006).

[7] S. N. Dorogovtsev, A. V. Goltsev and J. F. F. Mendes. Rev. Mod. Phys. **80**, 1275–1335 (2008).

[8] S.H. Strogatz, Nature **410,** 268 (2001).

[9] A. Arenas, A. Díaz-Guilera, J. Kurths, Y. Moreno and C. S. Zhou. Phys. Rep. **469**, 93–153 (2008).

[10] Y. Moreno and A.F. Pacheco, Europhys. Lett. **68,** 603 (2004).

[11] A. Arenas, A. Díaz-Guilera and C.J. Pérez-Vicente, Phys. Rev. Lett. **96**, 114102 (2006).

[12] J. Gómez-Gardeñes, Y. Moreno and A. Arenas, Phys. Rev. Lett. **98**, 034101 (2007).

[13] I. Lodato, S. Boccaletti and V. Latora, Europhys. Lett. **78**, 28001 (2007).

[14] J. Gómez-Gardeñes, S. Gómez, A. Arenas and Y. Moreno. Phys. Rev. Lett. **106**, 128701 (2011).

[15] T. Nishikawa, A.E. Motter, Y.-C. Lai and F.C. Hoppensteadt, Phys. Rev. Lett. **91**, 014101 (2003).

[16] M. Chavez, D.-U. Hwang, A. Amann, H.G.E. Hentschel and S. Boccaletti, Phys. Rev. Lett. **94**, 218701 (2005).

[17] C. Zhou, A.E. Motter and J. Kurths, Phys. Rev. Lett. **96**, 034101 (2006).

[18] D. Gfeller, P. De Los Rios, Phys. Rev. Lett. **100**, 174104 (2008).

[19] C. Zhou and J. Kurths, Phys. Rev. Lett. **96,** 164102 (2006).

[20] F. Sorrentino and E. Ott, Phys. Rev. Lett. **100,** 114101 (2008).

[21] T. Aoki and T. Aoyagi, Phys. Rev. Lett. **102,** 034101 (2009).

[22] R. Gutierrez, A. Amann, S. Assenza, J. Gómez-Gardeñes, V. Latora and S. Boccaletti, Phys. Rev. Lett. **107**, 234103 (2011).

[23] Y. Kuramoto, Lect. Notes in Physics **30**, 420 (1975).

[24] J.A. Acebrón, L.L. Bonilla, C.J. Pérez-Vicente, F. Ritort and R. Spigler Rev. Mod. Phys. **77**, 137 (2005).

[25] A. Bergner, M. Frasca, G. Sciuto, A. Buscarino, E. J. Ngamga, L. Fortuna and J. Kurths, Phys. Rev. E **85**, 026208 (2012).

[26] J. Gómez-Gardeñes and Y. Moreno, Phys. Rev. E **73**, 056124 (2006).

[27] The value of k^* is set so that the percentage of hubs is around the 20% of the total number of nodes in the network.